Eliminating molecular-alignment dephasing with a phase-modulated femtosecond laser pulse

Yunxia Huang,[1,2] Huajie Chen,[1] Guizhen Liu,[1] and Shuwu Xu[1,2,*]
[1]*School of Science, Nantong University, Nantong 226019, China*
[2]*Research Center for Quantum Physics and Materials, Nantong University, Nantong 226019, China*

(Received 1 February 2023; accepted 26 April 2023; published 11 May 2023)

Alignment dephasing caused by centrifugal distortion is a significant effect accompanying laser-induced field-free molecular alignment. Centrifugal distortion is the manifestation of the intrinsic nonrigidity of molecules, which is especially prominent when molecules are excited to high angular velocities. In this work, we show that this type of dephasing can be almost completely eliminated by modulating the phase of the femtosecond laser pulse. Nearly perfect molecular alignment can be achieved as if the molecules were ideal rigid rotors. The dephasing effect can be cancelled in various time windows by tuning the modulation strength parameter. The dephasing cancellation mechanism is explained by considering the relative phases of the eigenstates forming the rotational wave packet. This work is of great significance to the experiment and dynamics studies of molecular alignment.

DOI: 10.1103/PhysRevA.107.053108

I. INTRODUCTION

In recent decades, advanced gas-phase experiments in molecular physics have required the ability to control molecular alignment. Various schemes for inducing molecular alignment were applied in studies of chemical reaction dynamics, high-order harmonic generation, surface processing, molecular rotational echoes, and so on [1–10]. Alignment is said to be created when a preferred direction within a molecular ensemble is defined with respect to a space-fixed axis. Among various methods that create molecular alignment, a strong, nonresonant, linearly polarized laser pulse has been shown to be the most versatile technique because the laser-molecule interaction energy is typically much larger than the rotational energy of the molecules [11,12]. There are two different ways to induce molecular alignment using a strong laser field [13]. One way is by using relatively long laser pulses with a duration greatly exceeding the molecular rotational period. The laser-molecule interaction results in so-called "pendular" states. The molecular ensemble returns smoothly to the isotropic angular distribution as the laser pulse slowly fades away [14]; the alignment proceeds adiabatically and is termed "adiabatic alignment." The other case, often called "nonadiabatic alignment," employs a laser pulse that turns on and off rapidly compared to the rotational period of the molecule. In this case, the laser-molecule interaction can be viewed as a "kick" that creates a coherent superposition of rotational eigenstates, i.e., a broad rotational wave packet. Different components of the wave packet accumulate phase during the field-free evolution [10,15]. Rephasing of the rotational wave packet components results in alignment revival. One of the important advantages of the nonadiabatic alignment is that it can be reconstructed under field-free conditions periodically at multiple revival times.

Based on the rigid rotor model, the field-free molecular alignment of a linear molecule perfectly recurs for a long time after the interaction. However, in real molecules of finite rigidity, the alignment gradually becomes distorted during its field-free evolutions [16]. The distortion is visible even during the first few alignment revivals in molecules with a long rotational period or at high rotational temperatures. The distortion manifests in multiple oscillations and weakening of the alignment signal. The deformation of the signal limits its further application. Rooted in the intrinsic properties of the rapidly spinning molecules, it is hard to eliminate the alignment distortion completely. Recently, it was demonstrated that the centrifugal distortion can be eliminated using rotational echoes [17].

In the past few decades, with the development of the ultrafast pulse-shaping technique, tailoring the laser pulse with spectral phase modulation has shown to be effective for manipulating the molecular alignment. Many schemes, such as periodic phase step modulation, V-style phase modulation, cubic phase modulation, or the optimized feedback strategy have been utilized to control the molecular alignment [18–25]. In previous studies, the cubic phase modulation has proved to be an effective method for manipulating the revival structure and enhancing the degree of the molecular alignment [21]. In this work, we further demonstrate that this type of phase-modulated laser pulse can be efficient in eliminating the centrifugal distortion caused alignment dephasing. We show that, for the first time, to our knowledge, the dephasing can be completely eliminated by the cubic phase tailored femtosecond laser pulse. By appropriately manipulating the phase modulation parameter, perfect molecular alignment as that of the laser-induced ideal rigid rotors can be realized at any time window.

II. THEORETICAL MODEL

A detailed description of the laser-induced nonresonant molecular alignment and the cubic phase modulation has been

*xsw@ntu.edu.cn

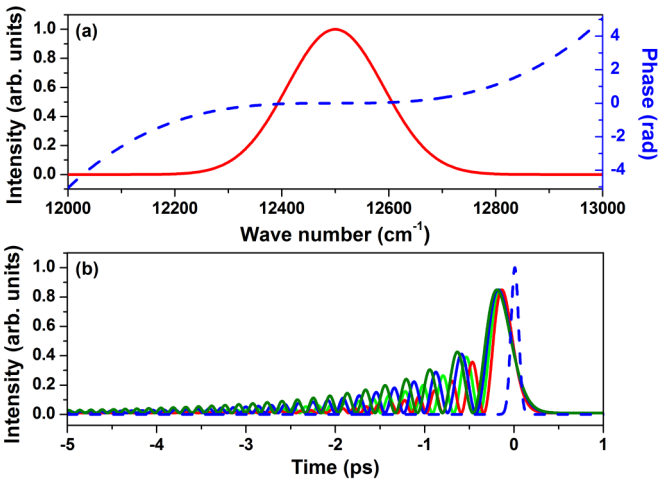

FIG. 1. (a) The Gaussian distribution of the 100-fs laser spectrum (red solid line) and the cubic phase modulation $\phi(\omega) = \alpha(\omega - \omega_0)^3$ with $\alpha = 1.5 \times 10^6$ fs^3 (blue dashed line). (b) The temporal intensity profile of the 100-fs transform-limited laser pulse (blue dashed line) and the shaped laser pulse by the cubic phase modulation with $\alpha = 1.0 \times 10^6$ fs^3 (red solid line), 1.5×10^6 fs^3 (green solid line), 2.0×10^6 fs^3 (blue solid line), and 2.5×10^6 fs^3 (olive solid line).

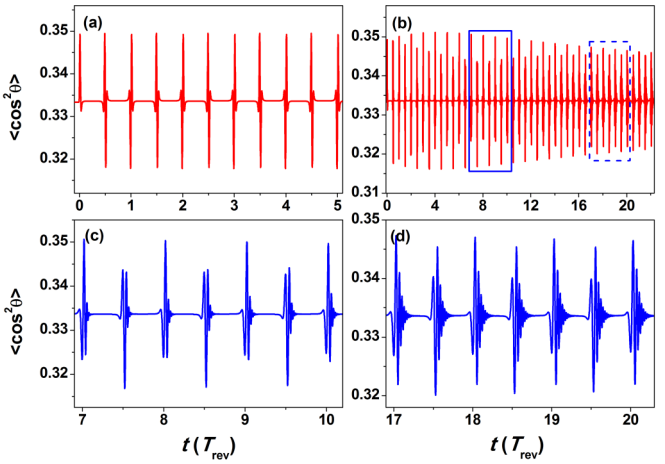

FIG. 2. Time-dependent molecular alignment of CO molecules induced by the transform-limited laser pulse with the model of (a) a rigid rotor and (b) a real rotor by considering the centrifugal distortion. (c) and (d), respectively, are the enlarged part of the solid and dashed rectangles shown in (b).

thoroughly introduced in many previous works and is briefly presented here. Consider an ensemble of linear molecules excited by a linearly polarized laser field

$$E(t) = E_0 f(t) \cos(\omega_0 t), \tag{1}$$

where $f(t)$ is the pulse envelope temporal profile with the expression

$$f(t) = \exp[(-2\ln 2)t^2/\sigma^2], \tag{2}$$

where E_0 is the laser field amplitude, ω_0 is the laser central frequency, and σ is the pulse duration. Laser-molecule interaction results in a torque on the molecules due to the molecular polarizability anisotropy $\Delta\alpha = \alpha_{||} - \alpha_\perp$. Here, $\alpha_{||}$ and $\alpha_\perp$ are the polarizability components parallel and perpendicular to the molecular axis, respectively. As a result, the molecules tend to align transiently along the laser polarization direction. Based on the rigid rotor model, the Hamiltonian describing the molecular rotational dynamics can be written as

$$\begin{aligned} H(t) &= E_J - V(t) \\ &= BJ(J+1) - (1/2)E^2(t)(\Delta\alpha\cos^2\theta + \alpha_\perp), \end{aligned} \tag{3}$$

where E_J and $V(t)$ are, respectively, the rotational energy and the laser field-molecule interaction energy; B is the rotational constant of the molecule; J is the quantum number of the rotational angular momentum; and θ is the angle between the molecular axis and the polarization direction of the laser field. The quantization of the rotational angular momentum manifests in periodic revivals with the rotational revival period $T_{\rm rev} = 1/(2Bc)$, where c is the light velocity in a vacuum. However, real molecules cannot be regarded as ideal rigid rotors in some cases. Another term, called "centrifugal distortion," should be considered, especially for high angular momentum (J). Thus the term of the rotational energy in Eq. (3) is rewritten as $E_J = BJ(J+1) - DJ^2(J+1)^2$, where D is the centrifugal distortion constant. The molecular alignment is usually characterized by the expectation value of $\cos^2\theta$ (i.e.,$\langle\cos^2\theta\rangle$) with

$$\langle\cos^2\theta\rangle = \langle\psi_{JM}|\cos^2\theta|\psi_{JM}\rangle, \tag{4}$$

where Ψ_{JM} is the rotational wave packet formed by the laser-molecule interaction, M is the magnetic quantum number, and the subscripts J and M label the initial rotational state. Notice that expectation values obtained for various initial states should be averaged over the Boltzmann distribution because, initially, the molecules are in thermal equilibrium [22–24].

The cubic spectral phase modulation function applied to the transform-limited laser pulse can be defined by

$$\phi(\omega) = \alpha(\omega - \omega_0)^3, \tag{5}$$

where α is the modulation depth [26]. Thus, the shaped laser pulse by the cubic phase modulation in frequency domain $E_s(\omega)$ can be written as $E_s(\omega) = E(\omega) \times \exp[i\phi(\omega)]$, where $E(\omega)$ is the Fourier transform of the unshaped laser field $E(t)$. The final shaped laser field $E_s(t)$ in the time domain can be given by the reverse Fourier transform of $E_s(\omega)$. Figure 1(a) shows the cubic spectral phase modulation in the frequency domain, and the temporal intensity profiles in the time domain with different modulation depths are shown in Fig. 1(b), together with the transform-limited femtosecond laser pulse as a comparison. One can see from Fig. 1(b) that a pulse train with increased intensity in the negative time delay can be formed by the cubic phase modulation. For the multiple subpulses, the intensity decreases while the pulse duration slightly increases compared to the transform-limited laser pulse. By monitoring the modulation depth α, both the intensity and the duration ratios between the subpulses can be slightly adjusted, as shown by the four colored solid lines in Fig. 1(b).

In our calculation, we use the CO molecule as an example and the molecular parameters are $B = 0.2039\,\text{cm}^{-1}$, $D = 6.1 \times 10^{-6}\,\text{cm}^{-1}$, $\Delta\alpha = \alpha_{||} - \alpha_\perp = 4.1\,\text{Å}^3$ [16,27]. Thus,

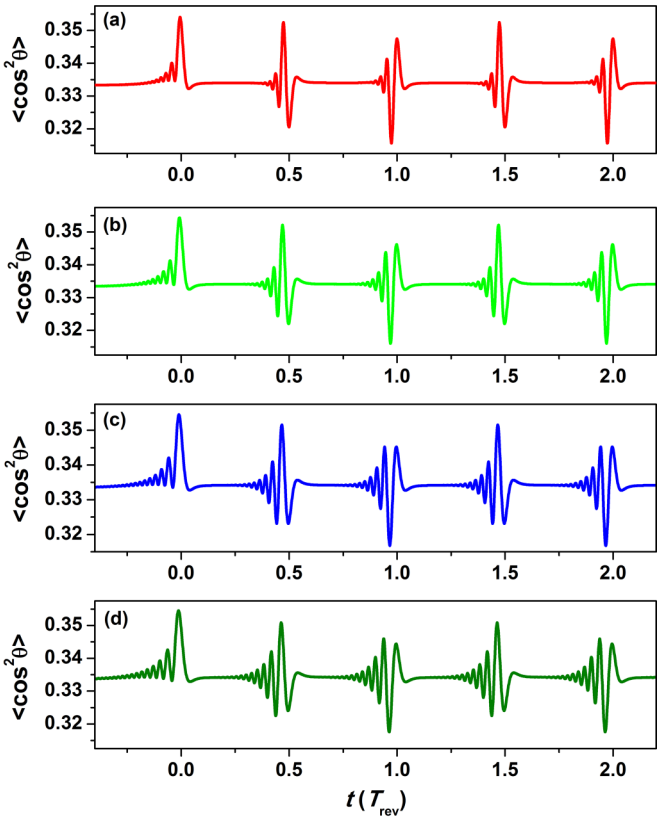

FIG. 3. Time-dependent molecular alignment of the CO rigid rotor induced by the cubic phase-shaped laser pulse with the phase modulation (a) $\alpha = 1.0 \times 10^6$ fs^3, (b) 1.5×10^6 fs^3, (c) 2.0×10^6 fs^3, and (d) 2.5×10^6 fs^3.

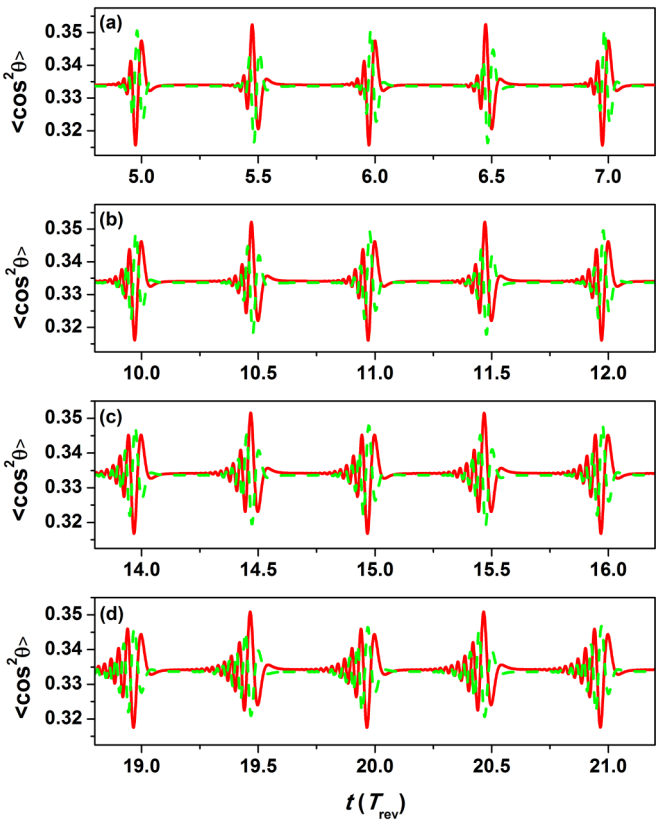

FIG. 4. Time-dependent molecular alignment of the CO rigid rotor induced by the cubic phase-shaped laser pulse with the phase modulation (a) $\alpha = 1.0 \times 10^6$ fs^3, (b) 1.5×10^6 fs^3, (c) 2.0×10^6 fs^3, and (d) 2.5×10^6 fs^3 as that shown in Fig. 3, but for different periodic revivals (solid lines), together with the mirror-symmetric molecular alignment of the same periodic revivals for a real rotor induced by the transform-limited laser pulse (dashed lines).

the revival period is $T_{\rm rev} = 1/(2Bc) = 8.64$ ps. The molecular rotational temperature is set to 300 K, and initial states with J up to $J = 50$ were included in our calculations. Parameters of the transform-limited laser pulse are set as follows: The carrier frequency is $\omega_0 = 12\,500\,{\rm cm}^{-1}$, the pulse duration is $\sigma = 100$ fs, and the peak intensity is $I = 1 \times 10^{13}$ W/cm^2.

III. RESULTS AND DISCUSSION

We first demonstrate in Fig. 2(a) the time-dependent molecular alignment of CO molecules assuming a rigid rotor model. The alignment signal including the centrifugal distortion effect is presented in Fig. 2(b). To observe the detail of the dephasing clearly, enlarged molecular alignment around the 7th to 10th and 17th to 20th periodic revivals are further illustrated in Figs. 2(c) and 2(d). One can see that, in contrast to the molecular alignment of a rigid rotor, where the alignment signals periodically reconstruct perfectly for a long time, alignment dephasing occurs after only few periodic revivals for a real rotor considered with the centrifugal distortion. Dephasing manifests in the decrease of the signal intensity and an increasing number of oscillations. As the molecular alignment evolves, the dephasing becomes more and more pronounced. According to previous work [16,17], the rotational wave packet created by field-molecule interaction can be expressed as

$$\psi_{JM}(t) = \sum_{J,M} A_{J,M}(t)|J, M\rangle, \tag{6}$$

where $A_{J,M}(t)$ is the expansion coefficients. Notice that the magnetic quantum number M is conserved in the linearly polarized laser field and omitted in the following discussions. Once created, a time-evolved rotational wave packet under field-free Hamiltonian can be written as

$$\psi_J(t) = \sum_J A_J e^{-i\hat{H}t/\hbar}|J\rangle = \sum_J A_J e^{-iE_J t/\hbar}|J\rangle, \tag{7}$$

with $E_J = BJ(J+1) - DJ^2(J+1)^2$. The expectation value of the alignment can be calculated considering the selection rule $J \to J' = J, J \pm 2$. The time-dependent alignment signals governed by $J \to J' = J \pm 2$ is of interest and is given by

$$\begin{aligned} S(t) &\propto \langle\psi_J(t)|\cos^2\theta|\psi_J(t)\rangle \\ &\propto \sum_J C_J \exp[-i(E_{J+2} - E_J)t/\hbar] + \text{c.c.} \end{aligned} \tag{8}$$

with $C_J \equiv A_J^* A_{J+2}\langle J|\cos^2\theta|J+2\rangle$ and $E_{J+2} - E_J = 2B(2J+3) - 4D(2J^3 + 9J^2 + 15J + 9)$. Here, the alignment signal from the transitions $J \to J' = J$ is independent of time

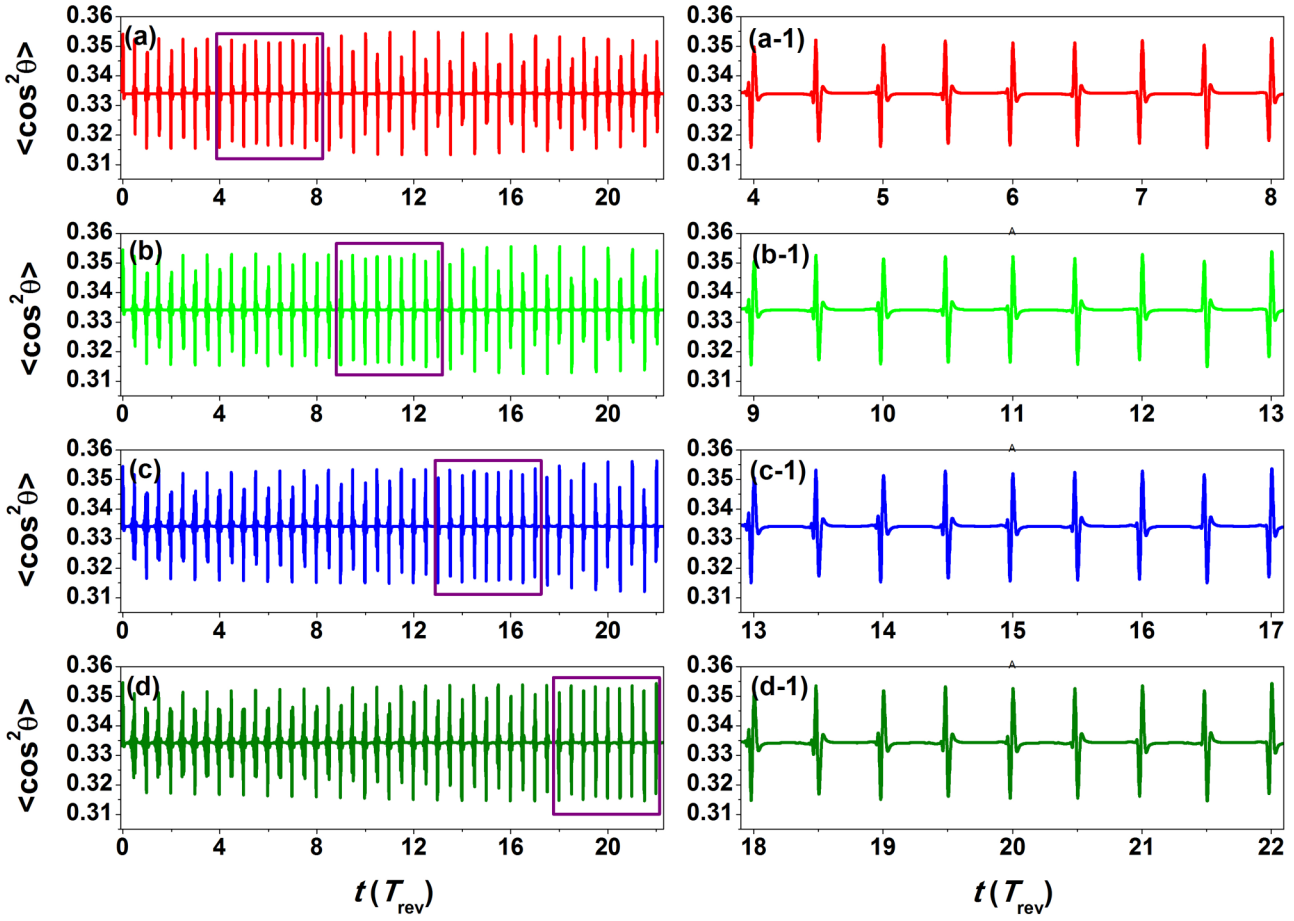

FIG. 5. Time-dependent molecular alignment of the CO real rotor induced by the cubic phase-shaped laser pulse with the modulation depth (a) $\alpha = 1.0 \times 10^6$ fs^3, (b) 1.5×10^6 fs^3, (c) 2.0×10^6 fs^3, and (d) 2.5×10^6 fs^3. The right column shows the corresponding enlarged rectangle parts of the left column.

because of $\Delta E_J = 0$ and is not considered. Thus, Eq. (8) can be rewritten as

$$S(t) \propto \sum_J C_J \exp[-i4\pi Bc(2J+3)t] \times \exp[i8\pi Dc(2J^3+9J^2+15J+9)t] + \text{c.c.} \quad (9)$$

Considering the molecular alignment at the full rotational revival period $t = nT_{\text{rev}} = n/(2Bc)$ (n is an integer), it is easy to obtain that the value of the first exponential term in Eq. (9) is 1. Thus, the alignment signals at full periodic revivals are given by the second exponential term and take the form

$$S(nT_{\text{rev}}) \propto \sum_J C_J \exp[i4\pi n(D/B) \times (2J^3+9J^2+15J+9)] + \text{c.c.} \quad (10)$$

It is the phase in the exponential term of Eq. (10) that causes the alignment signal distortion with time.

Eliminating the intrinsic dephasing caused by centrifugal distortion is a challenging and open problem in experiments on laser-induced molecular alignment. The multiple subpulses' structure of the shaped laser pulse by the cubic phase modulation shown in Fig. 1(b), which can further induce multiple oscillations of the molecular alignment, implies it might be efficient to resolve this problem. Figure 3 shows time-evolved molecular alignment of the CO rigid rotor induced by the cubic phase-shaped laser pulse with four different modulation depths: $\alpha = 1.0 \times 10^6$ fs^3, 1.5×10^6 fs^3, 2.0×10^6 fs^3, and 2.5×10^6 fs^3. It is displayed in Fig. 3 that similar oscillations of the alignment signal occur during each periodic revival as that in the alignment dephasing. The oscillation is determined by the modulation depth, i.e., by the multiple subpulses' structure of the shaped excitation pulse. However, in contrast to alignment dephasing, where the signal oscillation takes place after each periodic revival, the oscillation occurs before the recurrence of the molecular alignment in the rigid rotor cases induced by a cubic phase-shaped laser pulse. It is known that nonadiabatic laser excitation leaves the molecule in a superposition of rotational states, i.e., the laser pulse creates a broad rotational wave packet. A particular phase relation between different components of the wave packet is necessary to induce a significant degree of molecular alignment. That is, different signal structures of the molecular alignment presented in Fig. 3 by varying the modulation depth originate from different phase relations between the wave packets. Therefore, we can reasonably infer that, if the phase relation between the rotational wave packets of the molecular alignment shown in Fig. 3 is exactly equal to the opposite phase of the alignment dephasing demonstrated in Eq. (10),

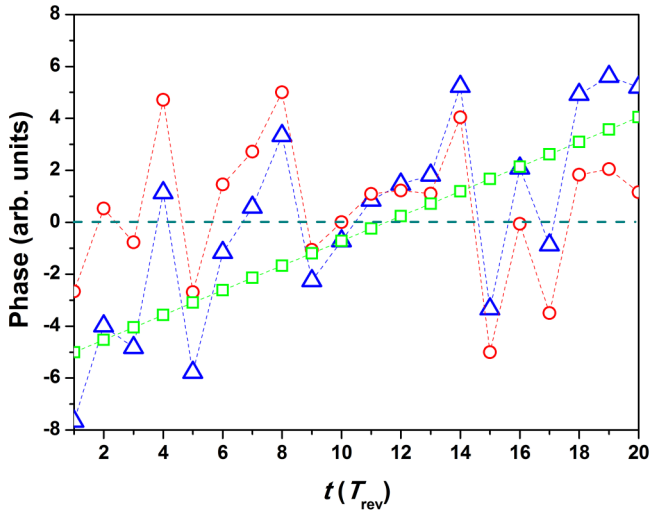

FIG. 6. Time-dependent phases of the full rotational revival periods for the molecular alignment of a rigid rotor induced by the cubic phase-shaped laser pulse with the modulation depth $\alpha = 1.5\times10^6$ fs^3 (red circles) and for the centrifugal distortion (green squares) in Eq. (10), together with the sum of both (blue triangles). The dashed olive line shows the relative zero phase.

the dephasing is expected to be eliminated because of the phases' cancellation. In other words, as long as the alignment structures of a rigid rotor excited by the cubic phase-shaped laser pulse and the dephasing-induced signal oscillations of a real molecule excited by the transform-limited laser pulse are exactly symmetric to the central position of a particular periodic revival, we can expect to realize the elimination of the dephasing by the cubic phase modulation.

Figure 4 demonstrates the time-dependent molecular alignment of the CO rigid rotor induced by the cubic phase-shaped laser pulse with four different phase modulation depths as that shown in Fig. 3, but for the revival periods of 5th–7th, 10th–12th, 14th–16th, and 19th–21st, respectively, together with the mirror-symmetric molecular alignment of the same periodic revivals for a real rotor induced by the transform-limited laser pulse. One can see that the alignment structures of the two cases, to some extent, are perfectly symmetric around the corresponding periodic revivals. According to the previous analysis, we can expect the dephasing to be eliminated by exciting a real molecule with a cubic phase-tailored laser pulse, and the results are presented in Fig. 5. By selecting the appropriate modulation parameters, nearly perfect molecular alignment as that of a rigid rotor is obtained for almost all the revival periods of 4th–22nd, as displayed in Fig. 5(a-1)–(d-1). It demonstrates that this strategy provides an effective method for eliminating the centrifugal distortion-induced dephasing for all the revival periods of the molecular alignment. However, one can see in time windows other than those shown in Fig. 5(a-1)–(d-1), the alignment signal during subsequent revivals looks distorted. It is clear that, for a particular modulation depth α, the elimination of the dephasing only occurs within several periodic revivals. On a very long timescale, alignment dephasing appears again. The elimination of the dephasing in a rather long time window still requires further investigation.

Finally, we further analyze the elimination of the dephasing from the perspective of phase superposition. As discussed earlier, it is the phase cancellation for all components of the rotational wave packet between the first term that depends on C_J (including some other omitting terms), and the second term that depends on D in Eq. (10) that results in the elimination of the dephasing. It is observed from Eq. (10) that the phase depends on C_J can be expressed by that of the molecular alignment of a rigid rotor induced by the cubic phase-shaped laser pulse. Figure 6 presents the calculated results of the two phases and their sum, i.e., superposition, with respect to the time-dependent full rotational revival periods for one of the used modulation depths, $\alpha = 1.5 \times 10^6$ fs^3, as an example. One can see that there is no clear pattern for the change of the sum phase except for those periodic revivals near the 10th–12th, where the corresponding sum phase changes around zero. Obviously, it is consistent with the simulation results for the same modulation depth shown in Fig. 5(b-1) and verifies our previous analysis.

IV. CONCLUSION

To conclude, we proposed a robust strategy to eliminate the centrifugal distortion-caused dephasing of the molecular alignment by tailoring the femtosecond laser pulse with the cubic phase modulation. Perfect molecular alignment can be reconstructed as that of the rigid rotor at any periodic revival by manipulating the phase modulation parameter. We show that this elimination of the dephasing originates from the cancellation of the two opposite phases, i.e., the phase between the rotational wave packets of the molecular alignment and the accumulated phase of the alignment dephasing. Although the study is limited to the alignment of the linear molecules, the results can be extended to the molecular orientation and to other complicated molecules, such as symmetric top molecules. This work provides a simple approach to visualize the connection between the rotational wave packets and corresponding coherences. The result is helpful in the experiment of molecular alignment and orientation, and deepens our understanding of the dephasing.

ACKNOWLEDGMENT

This work is supported by the National Natural Science Foundation of China (Grant No. 12004199).

[1] Y.- P. Chang, K. Długołecki, J. Küpper, D. Rösch, D. Wild, and S. Willitsch, Specific chemical reactivities of spatially separated 3-aminophenol conformers with cold Ca^+ ions, Science **342**, 98 (2013).

[2] I. V. Litvinyuk, K. F. Lee, P. W. Dooley, D. M. Rayner, D. M. Villeneuve, and P. B. Corkum, Alignment-Dependent Strong Field Ionization of Molecules, Phys. Rev. Lett. **90**, 233003 (2003).

[3] T. Kanai, S. Minemoto, and H. Sakai, Ellipticity Dependence of High-Order Harmonic Generation from Aligned Molecules, Phys. Rev. Lett. **98**, 053002 (2007).

[4] S. Haessler, J. Caillat, W. Boutu, C. Giovanetti-Teixeira, T. Ruchon, T. Auguste, Z. Diveki, P. Breger, A. Maquet, B. Carre, R. Taïeb, and P. Salières, Attosecond imaging of molecular electronic wavepackets, Nat. Phys. **6**, 200 (2010).

[5] M. Li, G. Jia, and X. Bian, Alignment dependent ultrafast electron-nuclear dynamics in molecular high-order harmonic generation, J. Chem. Phys. **146**, 084305 (2017).

[6] P. Rotter, B. A. J. Lechner, A. Morherr, D. M. Chisnall, D. J. Ward, A. P. Jardine, J. Ellis, W. Allison, B. Eckhardt, and G. Witte, Coupling between diffusion and orientation of pentacene molecules on an organic surface, Nat. Mater. **15**, 397 (2016).

[7] G. J. Simpson, V. Garcia-Lopez, A. D. Boese, J. M. Tour, and L. Grill, How to control single-molecule rotation, Nat. Commun. **10**, 4631 (2019).

[8] G. Karras, E. Hertz, F. Billard, B. Lavorel, J.- M. Hartmann, O. Faucher, E. Gershnabel, Y. Prior, and I. S. Averbukh, Orientation and Alignment Echoes, Phys. Rev. Lett. **114**, 153601 (2015).

[9] L. Xu, I. Tutunnikov, L. Zhou, K. Lin, J. Qiang, P. Lu, Y. Prior, I. S. Averbukh, and J. Wu, Echoes in unidirectionally rotating molecules, Phys. Rev. A **102**, 043116 (2020).

[10] S. Xu, G. Liu, and Y. Huang, Creating alignment echoes using a phase-shaped femtosecond laser pulse, J. Phys. B At. Mol. Opt. Phys. **55**, 155401 (2022).

[11] H. Stapelfeldt and T. Seideman, Colloquium: Aligning molecules with strong laser pulses, Rev. Mod. Phys. **75**, 543 (2003).

[12] T. Seideman and E. Hamilton, Nonadiabatic alignment by intense pulses: Concepts, theory, and directions, Adv. At. Mol. Opt. Phys. **52**, 289 (2005).

[13] R. Torres, R. de Nalda, and J. P. Marangos, Dynamics of laser-induced molecular alignment in the impulsive and adiabatic regimes: A direct comparison, Phys. Rev. A **72**, 023420 (2005).

[14] J. E. Szekely and T. Seideman, Alignment Thresholds of Molecules, Phys. Rev. Lett. **129**, 183201 (2022).

[15] Y. Gao, C. Wu, N. Xu, G. Zeng, H. Jiang, H. Yang, and Q. Gong, Manipulating molecular rotational wave packets with strong femtosecond laser pulses, Phys. Rev. A **77**, 043404 (2008).

[16] Y. Huang, G. Liu, and S. Xu, Rotational dephasing of the molecular alignment by centrifugal distortion, Chin. Opt. Lett. **20**, 100005 (2022).

[17] D. Rosenberg, R. Damari, S. Kallush, and S. Fleischer, Rotational echoes: Rephasing of centrifugal distortion in laser induced molecular alignment, J. Phys. Chem. Lett. **8**, 5128 (2017).

[18] C. P. Koch, M. Lemeshko, and D. Sugny, Quantum control of molecular rotation, Rev. Mod. Phys. **91**, 035005 (2019).

[19] M. Renard, E. Hertz, S. Guerin, H. R. Jauslin, B. Lavorel, and O. Faucher, Control of field-free molecular alignment by phase-shaped laser pulses, Phys. Rev. A **72**, 025401 (2005).

[20] O. Ghafur, A. Rouzee, A. Gijsbertsen, W. K. Siu, S. Stolte, and M. J. J. Vrakking, Impulsive orientation and alignment of quantum-state-selected NO molecules, Nat. Phys. **5**, 289 (2009).

[21] S. Zhang, C. Lu, J. Shi, T. Jia, Z. Wang, and Z. Sun, Field-free molecular alignment by shaping femtosecond laser pulse with cubic phase modulation, Phys. Rev. A **84**, 013408 (2011).

[22] S. Zhang, C. Lu, T. Jia, Z. Sun, and J. Qiu, Field-free molecular alignment control by phase-shaped femtosecond laser pulse, J. Chem. Phys. **135**, 224308 (2011).

[23] S. Xu, Y. Yao, C. Lu, J. Ding, T. Jia, S. Zhang, and Z. Sun, Manipulating field-free molecular alignment by V-shaped femtosecond laser pulses, Phys. Rev. A **89**, 053420 (2014).

[24] Y. Huang, S. Xu, and S. Zhang, Selective excitation and control of the molecular orientation by a phase-shaped laser pulse, RSC Adv. **6**, 100295 (2016).

[25] Y. Huang and S. Xu, Controlling population of the molecular rotational state and the alignment theoretically by tailored femtosecond laser pulse, R. Soc. Open Sci. **5**, 171502 (2018).

[26] U. Lev, L. Graham, C. B. Madsen, I. Ben-Itzhak, B. D. Bruner, B. D. Esry, H. Frostig, O. Heber, A. Natan, V. S. Prabhudesai, D. Schwalm, Y. Silberberg, D. Strasser, I. D. Williams, and D. Zajfman, Quantum control of photodissociation using intense, femtosecond pulses shaped with third order dispersion, J. Phys. B At. Mol. Opt. Phys. **48**, 201001 (2015).

[27] NIST, Molecular microwave spectral databases, https://physics.nist.gov/PhysRefData/MolSpec.